Supplementary Information (SI) for Physical Chemistry Chemical Physics.
This journal is © the Owner Societies 2024

Supporting Information

Structural characterization of $Li_2(Mg_xZn_{1-x})_2W_2O_9$ for bluish-white luminescence in rare earth-free tungstate phosphors

Jing Xie [1], Liang Li [1,5], Yue Zhong [1], Tao Su [1], Wenming Wang [1], Yan Pan [2], Xiantao Wei [3], Yong Li [1,4*]

1. *School of Microelectronics & Data Science, Anhui University of Technology, Maanshan 243000, China*
2. *Analysis and Testing Central Facility, Anhui University of Technology, Maanshan 243000, China.*
3. *Physics Experiment Teaching Center, School of Physical Sciences, University of Science and Technology of China, Hefei 230026, China*
4. *Anhui Research Center of Generic Technology in New Display Industry, Hefei 230009, PR China*
5. *School of Physics and Optoelectronics, South China University of Technology, Guangdong 510640, China*

*Email: yongli@ahut.edu.cn;

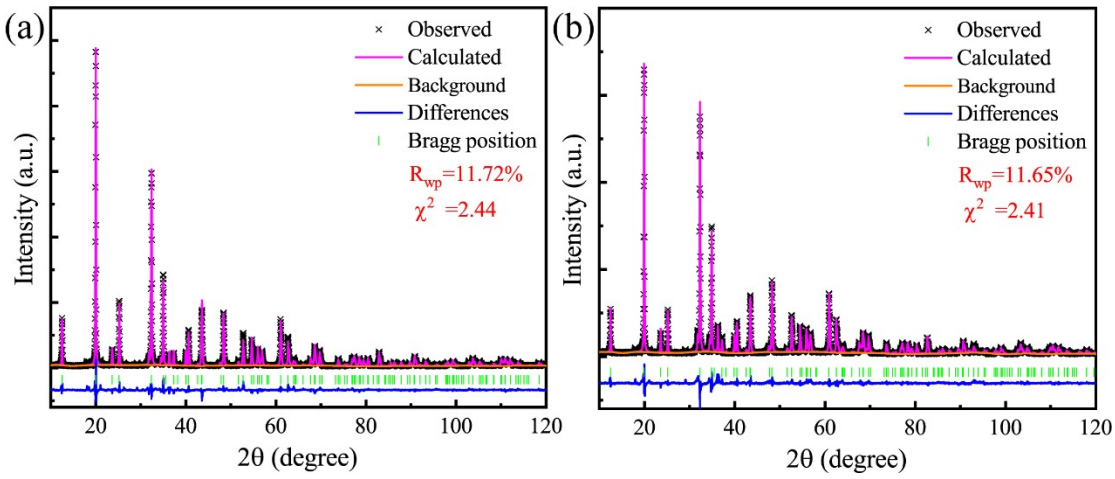

Fig. S1 (a) Rietveld refinement patterns of $Li_2(Mg_{0.5}Zn_{0.5})_2W_2O_9$ samples. (b) Rietveld refinement patterns of $Li_2Zn_2W_2O_9$ samples.

Fig. S1 illustrates the Rietveld refinement patterns of $Li_2(Mg_{0.5}Zn_{0.5})_2W_2O_9$ and $Li_2Zn_2W_2O_9$ samples. Good R_{wp} and χ^2 values were obtained from the refinements of sample XRD profiles. This indicates that the Rietveld method is successfully used to modify the crystal structures.

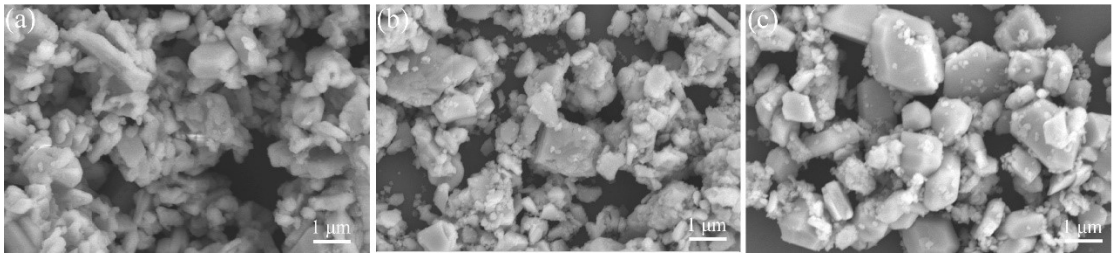

Fig. S2 SEM image of (a) $Li_2Mg_2W_2O_9$, (b) $Li_2(Mg_{0.5}Zn_{0.5})_2W_2O_9$, and (c) $Li_2Zn_2W_2O_9$ samples at the same magnification.

Fig. S2 illustrates the SEM image of the $Li_2Mg_2W_2O_9$, $Li_2(Mg_{0.5}Zn_{0.5})_2W_2O_9$, and $Li_2Zn_2W_2O_9$ samples at the same magnification. From the images, it can be observed that the particle size of the phosphor gradually increases with Zn^{2+} doping content.

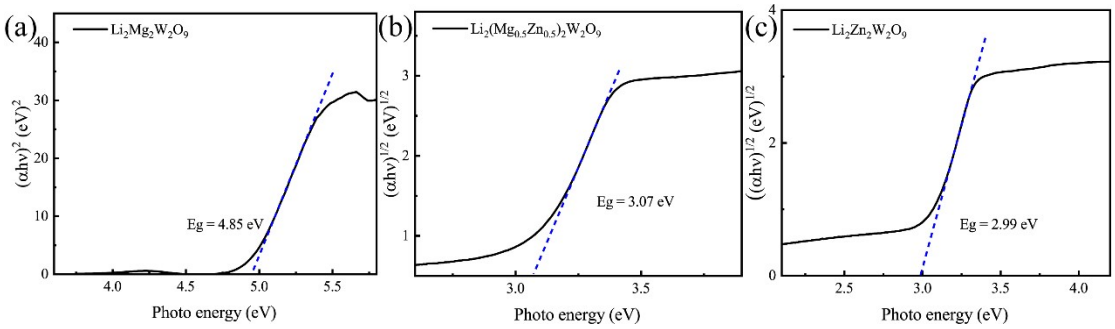

Fig. S3 The Kubelka−Munk spectra for the band gap energy calculation of $Li_2M_2W_2O_9$ (M = Mg, $Mg_{0.5}Zn_{0.5}$, and Zn).

Fig. S3 illustrates the curve of $[\alpha hv]^n$ versus hv. The calculated E_g values of the $Li_2M_2W_2O_9$ (M = Mg, $Mg_{0.5}Zn_{0.5}$, and Zn) phosphor are 4.85 eV, 3.07 eV, and 2.99 eV, respectively.

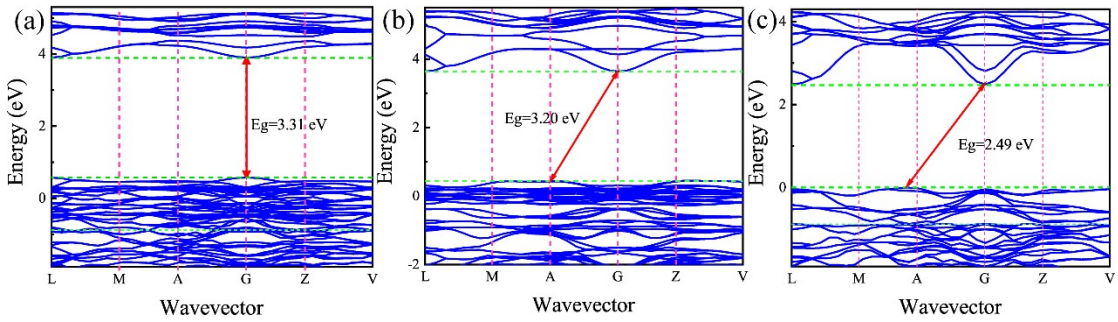

Fig. S4 Calculation of the energy band structure of $Li_2M_2W_2O_9$ (M = Mg, $Mg_{0.5}Zn_{0.5}$, and Zn).

The energy band structures of the $Li_2M_2W_2O_9$ (M = Mg, $Mg_{0.5}Zn_{0.5}$, and Zn) matrix were calculated by DFT from the Cambridge Serial Total Energy Package (CASTEP) codes. To improve the accuracy of the calculations, the Perdew–Burke–Ernzerhof (PBE) function of generalized gradient approximation with Hubbard U-values (GGA + U) was used. The theoretical value of E_g determined by density functional theory calculations are 3.31 eV, 3.20 eV, and 2.49 eV, respectively.

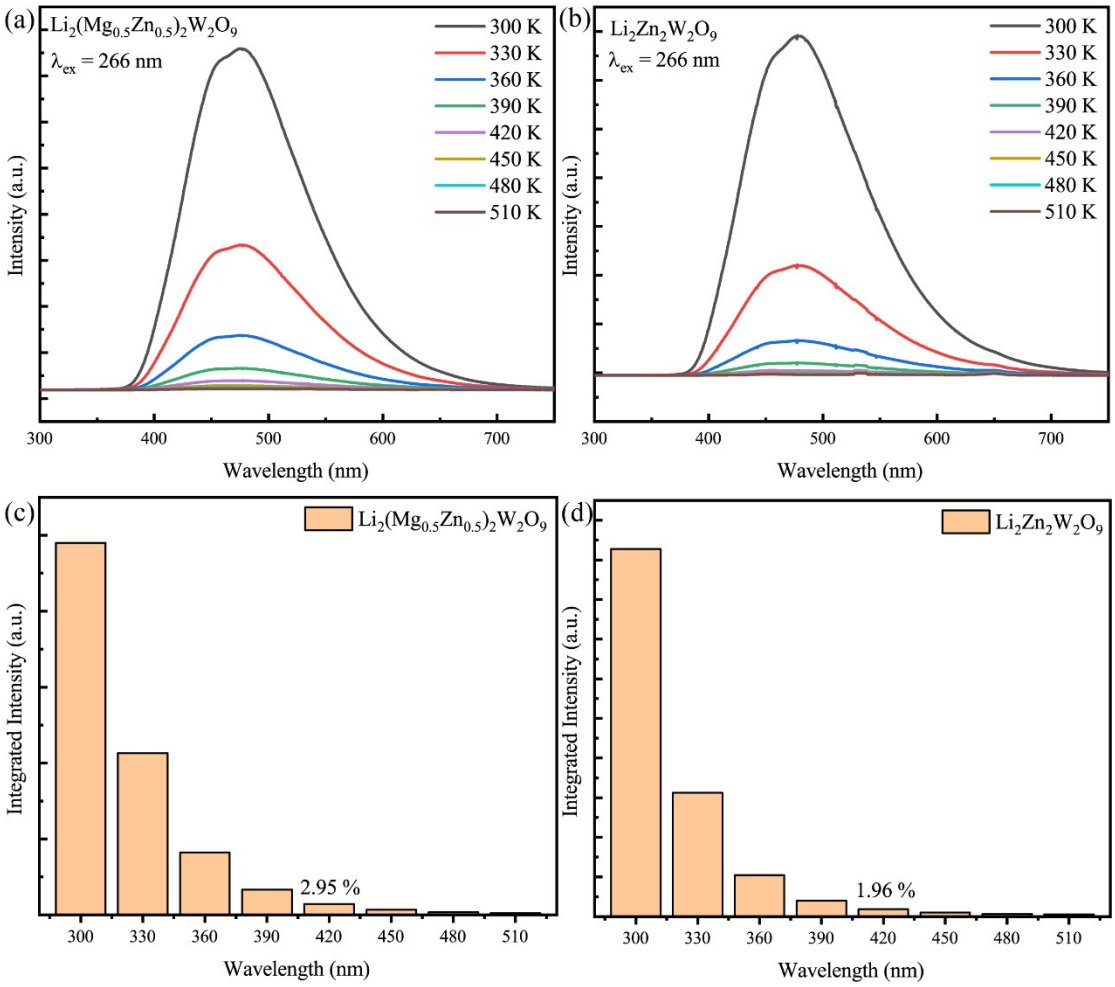

Fig. S5 The PL spectra and histograms with different temperatures of the $Li_2(Mg_{0.5}Zn_{0.5})_2W_2O_9$ and $Li_2Zn_2W_2O_9$ phosphors

The thermal dependence of the PL spectra for the $Li_2(Mg_{0.5}Zn_{0.5})_2W_2O_9$ and $Li_2Zn_2W_2O_9$ phosphor were measured from 300 to 540 K under excitation at 266 nm. No significant differences in the shape of the PL spectra are observed with increasing temperature, but a substantial decrease in PL intensity is observed for the samples. The integrated intensity histogram in Fig. S5(c, d) visualizes the trend of the PL intensity as a function of temperature. When the temperature was increased to 420 K, the PL intensity of the $Li_2(Mg_{0.5}Zn_{0.5})_2W_2O_9$ and $Li_2Zn_2W_2O_9$ samples is only 2.95% and 1.96% of the initial emission intensity at 300 K, respectively.

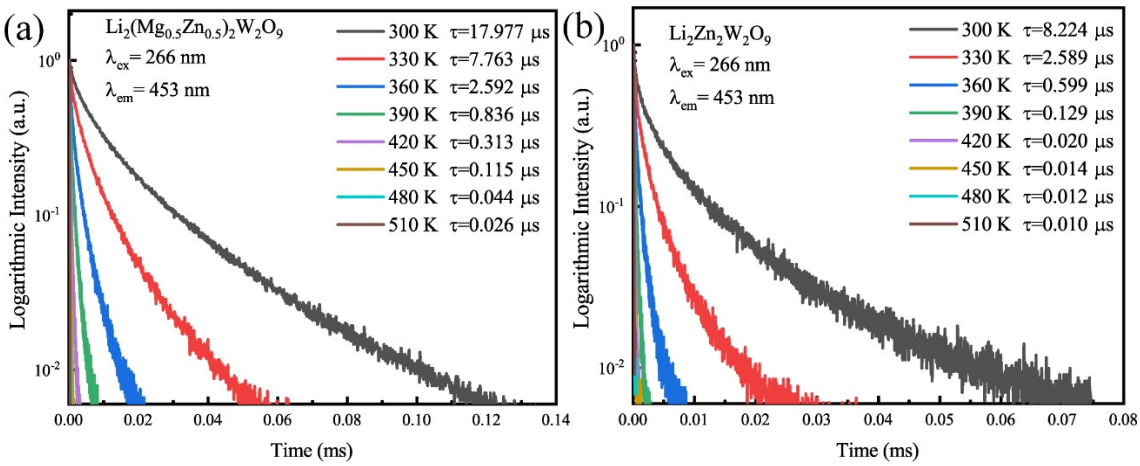

Fig. S6 The decay curves of red emission in $Li_2(Mg_{0.5}Zn_{0.5})_2W_2O_9$ and $Li_2Zn_2W_2O_9$ phosphors at different temperatures (300–510 K).

Fig. S6 illustrates the lifetime decay curves of the $Li_2(Mg_{0.5}Zn_{0.5})_2W_2O_9$ and $Li_2Zn_2W_2O_9$ samples at different temperatures. The lifetime data of samples are listed in Table S3. It can be observed that the lifetime of the samples gradually decreases as the temperature.

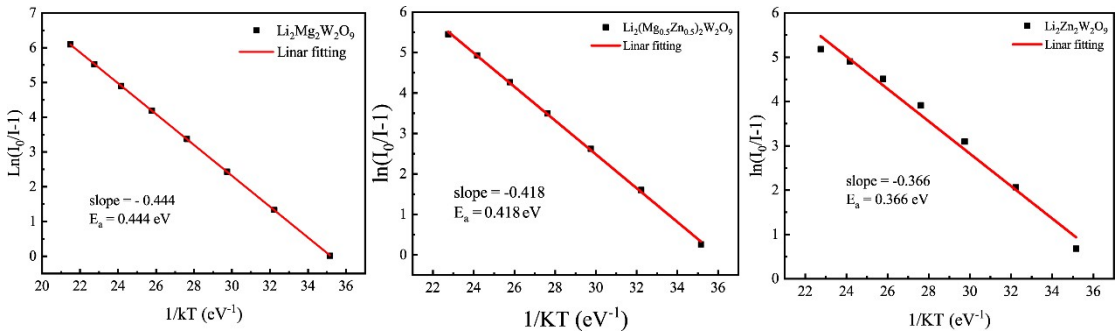

Fig. S7 Relationship between $Ln(I_0/I\text{-}1)$ and 1/kT in $Li_2M_2W_2O_9$ (M = Mg, $Mg_{0.5}Zn_{0.5}$, and Zn) phosphor.

Fig. S7 illustrates the relationship between $Ln(I_0/I\text{-}1)$ and 1/kT in $Li_2M_2W_2O_9$ (M = Mg, $Mg_{0.5}Zn_{0.5}$, and Zn) phosphor. The E_a corresponds to the slope of the $\ln[I_0/I(T)^{-1}]$ vs $[kT]^{-1}$ plot. By calculation, the values of E_a for the $Li_2M_2W_2O_9$ (M = Mg, $Mg_{0.5}Zn_{0.5}$, and Zn) phosphors are 0.444 eV, 0.418 eV, and 0.366 eV, respectively. The E_a of the samples decreased with increasing Zn^{2+} content.

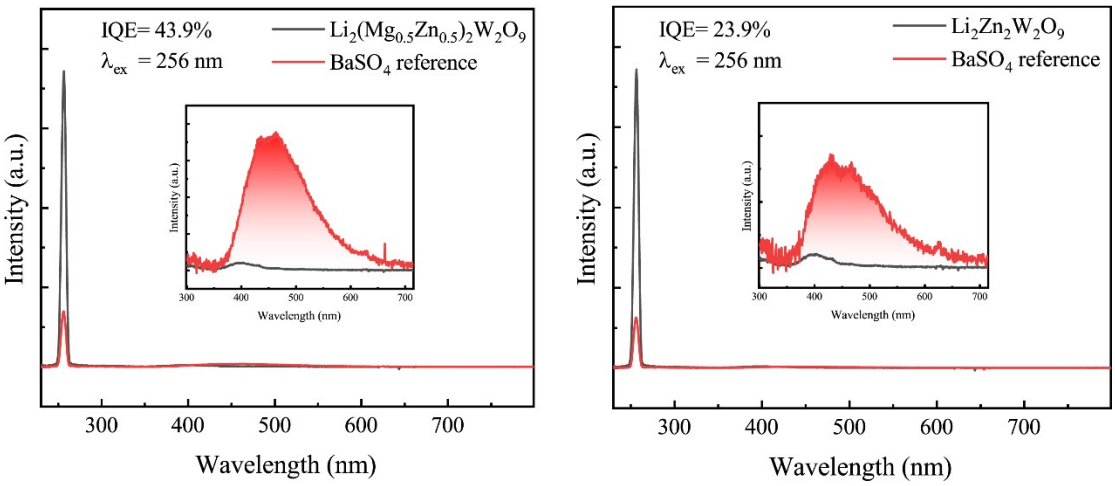

Fig. S8 (a) The IQE map of the $Li_2(Mg_{0.5}Zn_{0.5})_2W_2O_9$ phosphor sample. (b) The IQE map of the $Li_2Zn_2W_2O_9$ phosphor sample.

The IQE map of the $Li_2(Mg_{0.5}Zn_{0.5})_2W_2O_9$ and $Li_2Zn_2W_2O_9$ phosphor sample is exhibited in Fig. S8. Under 256 nm excitation, the internal quantum efficiencies of samples $Li_2(Mg_{0.5}Zn_{0.5})_2W_2O_9$ and $Li_2Zn_2W_2O_9$ are 43.9 % and 23.9 %, respectively.

Table. S1 The lifetime of the $Li_2(Mg_xZn_{1-x})_2W_2O_9$ (x = 0, 0.2, 0.5, 0.8, and 1) phosphor.

Phosphor	Lifetime (μs)
$Li_2Mg_2W_2O_9$	26.29
$Li_2(Mg_{0.8}Zn_{0.2})_2W_2O_9$	20.87
$Li_2(Mg_{0.5}Zn_{0.5})_2W_2O_9$	18.70
$Li_2(Mg_{0.2}Zn_{0.8})_2W_2O_9$	13.06
$Li_2Zn_2W_2O_9$	10.33

The lifetime of the $Li_2(Mg_xZn_{1-x})_2W_2O_9$ (x = 0, 0.2, 0.5, 0.8, and 1) phosphors is shown in Table S1. The Lifetime of samples decreases gradually with Zn^{2+} content.

Table. S2 Peak Wavelength and Energy of the PLE and PL Bands from the Gaussian Deconvolution

Band	Transition	$Li_2Mg_2W_2O_9$			$Li_2(Mg_{0.5}Zn_{0.5})_2W_2O_9$			$Li_2Zn_2W_2O_9$		
		Peak position (nm)	Energy(cm^{-1})	Energy (eV)	Peak position (nm)	Energy(cm^{-1})	Energy (eV)	Peak position (nm)	Energy(cm^{-1})	Energy (eV)
EX1	$^1A_1 \rightarrow {}^1T_1$	249	40092	4.97	250	39980	4.96	256	39002	4.84
EX2	$^1A_1 \rightarrow {}^1T_2$	209	47942	5.94	212	47260	5.86	212	47174	5.85
EM1	$^3T_1 \rightarrow {}^1A_1$	455	21967	2.72	470	21270	2.64	474	21097	2.62
EM2	$^3T_2 \rightarrow {}^1A_1$	425	23541	2.92	428	23376	2.90	431	23219	2.88

The PL and PLE spectra of the $Li_2M_2W_2O_9$ (M = Mg, $Mg_{0.5}Zn_{0.5}$, and Zn) phosphors were deconvolved using Gaussian functions to elucidate the detailed optical properties. Table S2 lists the deconvoluted peak positions. The emission and excitation wavelengths of the samples are red-shifted with increasing Zn^{2+} content.

Table. S3 The lifetime of the $Li_2M_2W_2O_9$ (M = Mg, $Mg_{0.5}Zn_{0.5}$, and Zn) phosphor at different temperatures

Temperature	Lifetime (μs)		
	$Li_2Mg_2W_2O_9$	$Li_2(Mg_{0.5}Zn_{0.5})_2W_2O_9$	$Li_2Zn_2W_2O_9$
300 K	30.098	17.977	8.224
330 K	15.686	7.763	2.589
360 K	6.488	2.592	0.699
390 K	2.364	0.836	0.129
420 K	0.816	0.313	0.020
450 K	0.340	0.115	0.014
480 K	0.156	0.044	0.012
510 K	0.070	0.026	0.010

Table. S3 illustrates the lifetime of the $Li_2M_2W_2O_9$ (M = Mg, $Mg_{0.5}Zn_{0.5}$, and Zn) phosphor at different temperatures. The luminescence lifetimes of all samples gradually decreased with the temperature. At the same temperature, the samples with more Zn^{2+} content have shorter lifetimes.

Table. S4 The calculated CIE coordinates (x, y) of $Li_2(Mg_xZn_{1-x})_2W_2O_9$ (x = 0, 0.2, 0.5, 0.8, and 1) phosphor.

phosphor	CIE coordinates (x, y)	
	x	y
$Li_2Mg_2W_2O_9$	0.19693	0.251
$Li_2(Mg_{0.8}Zn_{0.2})_2W_2O_9$	0.2053	0.26598
$Li_2(Mg_{0.5}Zn_{0.5})_2W_2O_9$	0.21001	0.27273
$Li_2(Mg_{0.2}Zn_{0.8})_2W_2O_9$	0.21577	0.28467
$Li_2Zn_2W_2O_9$	0.22806	0.29133

The calculated CIE coordinates (x, y) are shown in Table S4. The luminescent color of the phosphor is shifted from the deep blue to the light blue region with the increase of Zn content.